OPEN ACCESS

ORIGINAL RESEARCH

Metal artifact reduction for flat panel detector intravenous CT angiography in patients with intracranial metallic implants after endovascular and surgical treatment

Rastislav Pjontek,[1] Belgin Önenköprülü,[1] Bernhard Scholz,[2] Yiannis Kyriakou,[2] Gerrit A Schubert,[3] Omid Nikoubashman,[1,4] Ahmed Othman,[1] Martin Wiesmann,[1] Marc A Brockmann[1]

[1]Department of Diagnostic and Interventional Neuroradiology, University Hospital RWTH Aachen, Aachen, Germany
[2]Healthcare, Imaging & Therapy Division, Siemens AG, Forchheim, Germany
[3]Department of Neurosurgery, University Hospital RWTH Aachen, Aachen, Germany
[4]Institute of Neuroscience and Medicine 4, Medical Imaging Physics, Forschungszentrum Jülich, Jülich, Germany

Correspondence to
Professor Marc A Brockmann, Department of Diagnostic and Interventional Neuroradiology, University Hospital RWTH Aachen, Pauwelsstr 30, Aachen 52074, Germany; brockmann@gmx.de

RP and BÖ contributed equally.

Received 8 April 2015
Revised 8 July 2015
Accepted 13 July 2015
Published Online First 7 September 2015

ABSTRACT

Background Flat panel detector CT angiography with intravenous contrast agent injection (IV CTA) allows high-resolution imaging of cerebrovascular structures. Artifacts caused by metallic implants like platinum coils or clips lead to degradation of image quality and are a significant problem.

Objective To evaluate the influence of a prototype metal artifact reduction (MAR) algorithm on image quality in patients with intracranial metallic implants.

Methods Flat panel detector CT after intravenous application of 80 mL contrast agent was performed with an angiography system (Artis zee; Siemens, Forchheim, Germany) using a 20 s rotation protocol (200° rotation angle, 20 s acquisition time, 496 projections). The data before and after MAR of 26 patients with a total of 34 implants (coils, clips, stents) were independently evaluated by two blinded neuroradiologists.

Results MAR improved the assessability of the brain parenchyma and small vessels (diameter <1 mm) in the neighborhood of metallic implants and at a distance of 6 cm ($p<0.001$ each, Wilcoxon test). Furthermore, MAR significantly improved the assessability of parent vessel patency and potential aneurysm remnants ($p<0.005$ each, McNemar test). MAR, however, did not improve assessability of stented vessels.

Conclusions When an intravenous contrast protocol is used, MAR significantly ameliorates the assessability of brain parenchyma, vessels, and treated aneurysms in patients with intracranial coils or clips.

INTRODUCTION

Patients treated endovascularly (embolization, stenting) or by open surgery (clipping) for cerebrovascular pathologies such as aneurysms frequently undergo follow-up imaging.[1 2] Catheter angiography is considered the 'gold standard' for vessel imaging owing to its high temporal and spatial resolution, but it is associated with a low but still existing risk owing to its invasive character.[3] On the other hand, lower spatial resolution and beam hardening artifacts in CT imaging as well as susceptibility artifacts in MRI may reduce the assessability of these modalities, which are being otherwise frequently used for non-invasive follow-up.

During the past years flat panel detector CT within the angiography suite has increasingly been used to rule out peri-interventional complications such as intracranial hemorrhage or to visualize implanted materials, and also to serve as a non-invasive method for high-resolution imaging of cerebrovascular structures and pathologies during follow-up.[4–7] Since metal artifacts strongly limit the diagnostic value of follow-up studies after clipping or coiling, and also in other fields of radiology,[8 9] the introduction of algorithms for metal artifact reduction (MAR) was an important step forward in providing images of diagnostic value in patients with metallic implants.[10 11]

This work aimed at evaluating the efficacy of a MAR algorithm developed by the vendor of our flat panel angiographic C-arm system and provided as prototype software component. It consists of three correction steps, in two of which the metal-corrupted projection data are replaced by a non-linear interpolation method, which is a numerically adapted realization of Cauchy's integral formula. Finally, residual streaks are reduced by an optimization procedure.

MATERIALS AND METHODS

Patient selection

Retrospective analysis of patients for inclusion in the study was approved by the local ethics committee of the University Hospital of the RWTH Aachen. Between February 2013 and September 2013, flat panel detector CT angiography with intravenous contrast agent injection (IV CTA) was performed in 31 cases with intracranial metallic implants used for treatment of vascular pathologies in our institution. Four datasets were excluded owing to technical or procedural problems, such as insufficient contrasting of the intracranial vessels or paravasation of the contrast agent. Finally, 27 datasets from 26 patients (23 women and 3 men with a mean age of 55 years (range 19–86); one patient was examined twice) with a total of 34 intracranial implants were included in the study.

Intracranial aneurysms were treated by neurosurgical clipping (n=12), platinum coil embolization (n=12), stent-assisted platinum coil embolization (n=6), flow diversion (n=1), and embolization with an intra-aneurysmal flow diverter (n=1). In addition, two patients with intracranial stenosis underwent stent angioplasty. All IV CTA scans were performed routinely as a follow-up procedure after treatment of the respective vessel pathology.

To cite: Pjontek R, Önenköprülü B, Scholz B, *et al*. *J NeuroIntervent Surg* 2016;**8**:824–829.

J NeuroIntervent Surg: first published as 10.1136/neurintsurg-2015-011787 on 7 September 2015. Downloaded from http://jnis.bmj.com/ on July 7, 2022 by guest. Protected by copyright.

Imaging protocol

All images were obtained with a flat panel angiographic C-arm system (Artis zee biplane; Siemens Healthcare, Forchheim, Germany) using the embedded high-quality DynaCT protocol (Siemens Healthcare) with an acquisition range of 200° (matrix 1240×960, 0.4° angular increment) and 496 projections. In contrast to other studies, we used a 20 s rotation protocol after intravenous injection of 80 mL of iodinated contrast agent (Solutrast 300; Bracco, Konstanz, Germany) into the cubital vein (5.0 mL/s). The scan was started when contrast enhancement of the intracranial carotid arteries was observed using a bolus tracking technique (bolus monitoring at 1 image/s).

After image acquisition the raw data were transferred to a workstation (Syngo MM Workplace AXK1447; Siemens Healthcare) and the MAR algorithm was applied as described below. Apart from MAR, all parameters of uncorrected and corrected data were kept identical. The time required for post-processing was measured.

MAR algorithm

The MAR algorithm investigated in this work is a modification, and an extension, of a previously published MAR algorithm.[12 13] The algorithm consists of several steps. Initially, an uncorrected volume image is reconstructed from the measured data. By segmenting the metal objects in this volume a binary metal volume image is obtained. For each projection this binary volume is forward-projected to yield a binary projection image of metal regions on the detector in the respective position. The projection data contained in these metal regions are generated by rays through metal objects, and thus these data are responsible for the artifacts. The data along the metal region boundaries are used to replace these data by a non-linear interpolation procedure. The so-far corrected volume is used for a second, normalized MAR correction step.[14] This step includes, additionally, iterative improvements of the metal region boundaries in order to enhance consistency of the corrected data as a whole. The third and final step is to apply a procedure minimizing the total variation in order to reduce residual streaks.

Qualitative image evaluation and statistical analysis

All uncorrected and corrected data (ie, data before and after MAR) were assessed in randomized order separately by two neuroradiologists. Using a four-point Likert scale (1=excellent, 2=good, 3=limited, 4=insufficient) the raters assessed the depiction of brain parenchyma in the immediate neighborhood (<1 cm) of the implant and at a distance of 6 cm.

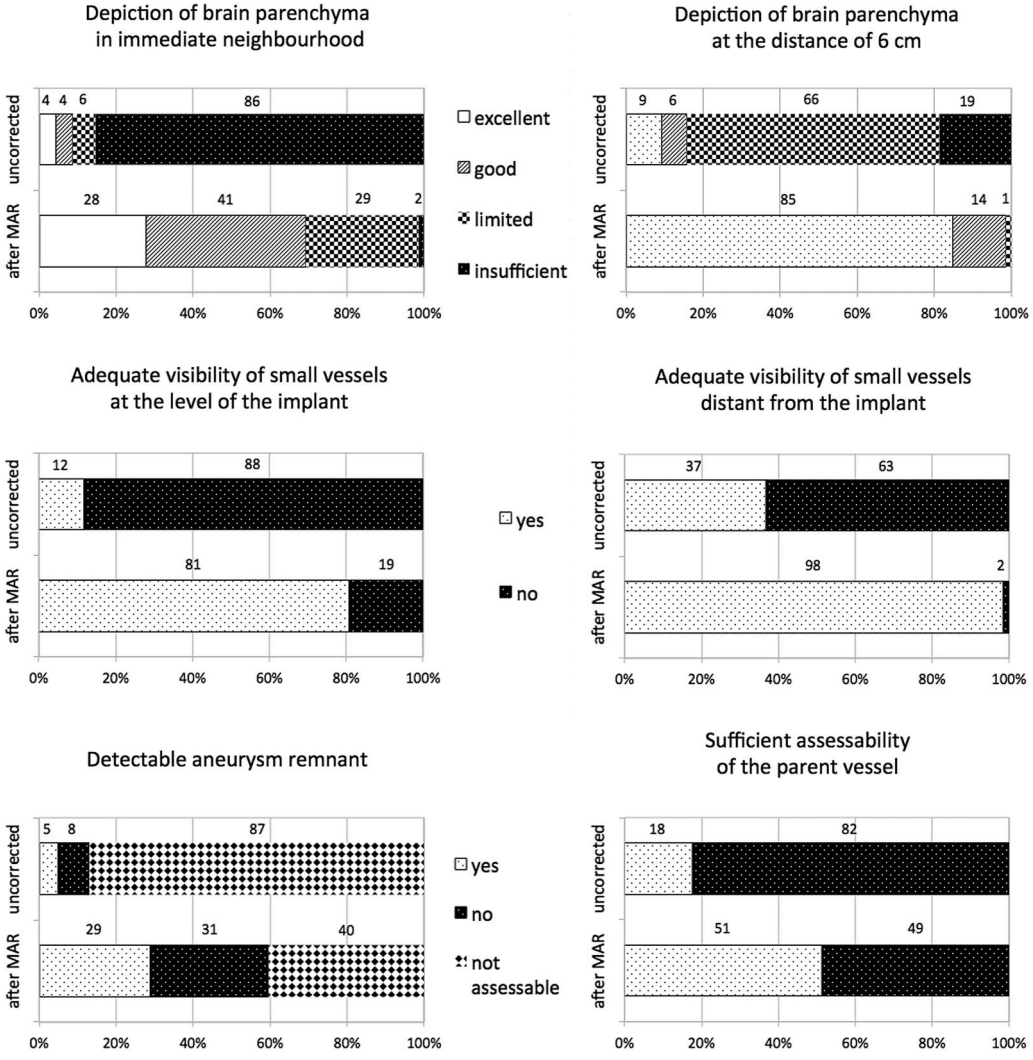

Figure 1 Graphic representation of image quality improvement in IV CT angiography datasets before and after metal artifact reduction (MAR) in patients with metallic intracranial implants: depiction of brain parenchyma in the upper row, adequate visibility of small vessels in the middle row, detectable aneurysm remnant and sufficient assessability of the parent vessel in the lower row.

J NeuroIntervent Surg: first published as 10.1136/neurintsurg-2015-011787 on 7 September 2015. Downloaded from http://jnis.bmj.com/ on July 7, 2022 by guest. Protected by copyright.

A dichotomous scoring model (1=positive answer, 2=negative answer) was applied to evaluate the adequate visibility of small vessels close to, and distant from, the implant, the assessability of contralateral vessels (ie, of the contralateral hemisphere or, for example, of the vertebrobasilar circulation for aneurysms of the anterior communicating artery and vice versa), of the parent vessel, and of potential aneurysm remnants. If applicable, the grade of aneurysm occlusion was quantified according to the modified Raymond classification.[1] In the presence of intracranial stents, in-stent stenosis in the middle and at the ends of the stent (1=positive answer, 2=negative answer, 3=not diagnostic owing to artifacts) as well as the parent vessel assessability (1=positive answer, 2=negative answer) were rated.

During the reading process, raters did not have access to patients' personal data or correction status. Interactive image manipulations, such as contrast and intensity adjustment of image window/level, setting of the slice thickness, zoom, pan, and rotation, were allowed. To reduce the recall bias, the reading process was extended to several weeks.

All statistical analyses were performed using SPSS 20 software (IBM Corp, Armonk, New York, USA). McNemar tests and Wilcoxon matched-pairs signed-rank tests were used for dichotomous questions and rating scale questions, respectively. The inter-rater reliability was assessed by a κ test. Results with a p value <0.05 were considered statistically significant.

RESULTS

Assessability of the brain parenchyma adjacent to the metallic implants in images before MAR was rated 'insufficient' or 'limited' in 31 cases (91%) and 'excellent' or 'good' in 3 cases (9%), whereas after MAR the brain parenchyma directly adjacent to the implant was characterized as excellent or good in 69% of datasets (Wilcoxon test, p<0.001). Likewise, the assessability of brain parenchyma at a distance of 6 cm away from the metallic implant improved significantly (Wilcoxon test, p<0.001) with the number of datasets being categorized as "excellent" increasing from 3 (9%) to 28 (85%). When the two major subgroups were analyzed separately (clipped patients and patients who underwent coiling without stenting; each group n=12), the assessability of the brain parenchyma remained significantly better after MAR (p<0.005).

Metal artifacts caused by the implants reduced the assessability of contralateral vessels in 72% of cases, whereas after MAR distant vessels were relevantly affected by metal artifacts in only one case (McNemar test, p<0.001). The assessability of small vessels in the neighborhood of the implant (<1 cm) and at a distance of 6 cm from the implant improved significantly from 12% to 81% and from 37% to 98%, respectively (McNemar test, p<0.001 each). Subgroup analysis (clipped patients and patients who underwent coiling without stenting; each group n=12) likewise showed significantly improved assessability of vascular structures after MAR (p<0.05). Only for the assessability of distant small vessels in one group (clipped aneurysms) one of the reviewers found that MAR provided no significant improvement (p=0.250). In this last group the reviewer judged assessability of vascular structures sufficient in most cases even before MAR.

Evaluation of the parent vessel was feasible in six uncorrected cases (18%), whereas MAR significantly increased the diagnostic assessability to 18 cases (McNemar test, p=0.004). Subgroup analysis (clipped patients and patients who underwent coiling without stenting; each group n=12) showed improvement of

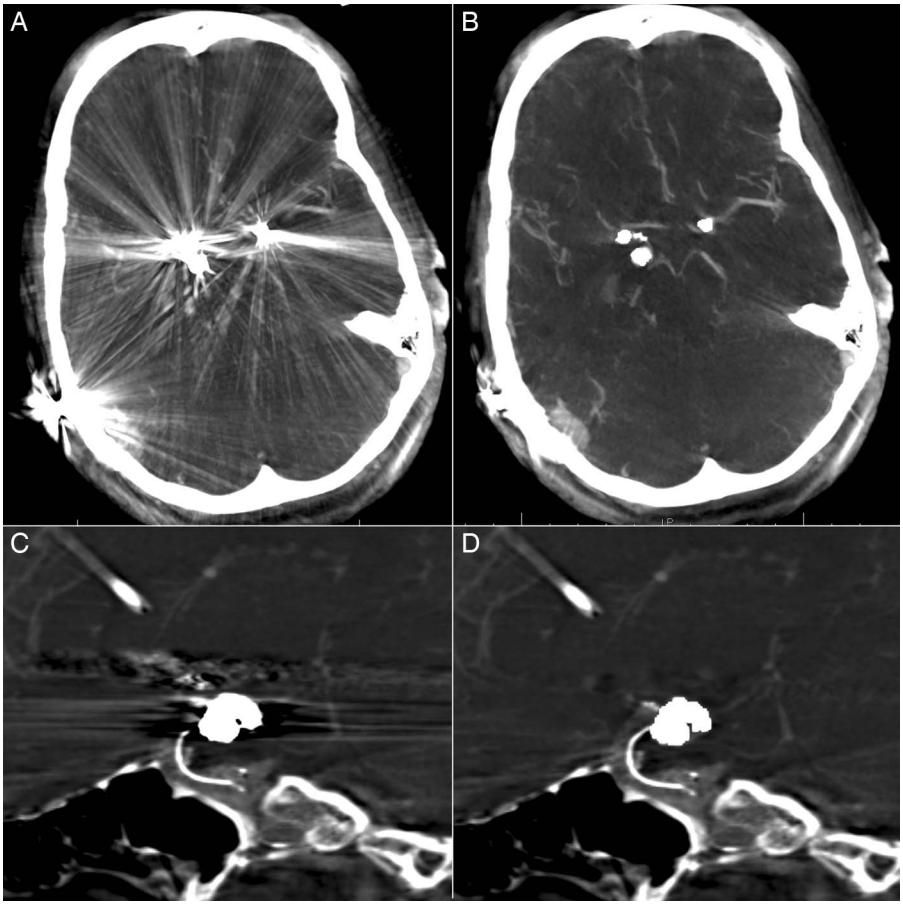

Figure 2 Axially (upper row) and sagittally (lower row) reconstructed IV CT angiograms after coil embolization of bilateral carotid T aneurysms and a right-sided posterior communicating artery aneurysm. Owing to peri-interventional coil dislocation two microstents were placed in the right internal carotid artery (C and D). The subarachnoid hemorrhage-related hydrocephalus was treated with ventriculo-peritoneal shunting. The extensive artifacts caused by the platinum coils and shunt valve (A and C) were remarkably reduced by metal artifact reduction (B and D). Consequently, the visibility of intracranial vessels, including the parent vessel (B and D), improved significantly.

J NeuroIntervent Surg: first published as 10.1136/neurintsurg-2015-011787 on 7 September 2015. Downloaded from http://jnis.bmj.com/ on July 7, 2022 by guest. Protected by copyright.

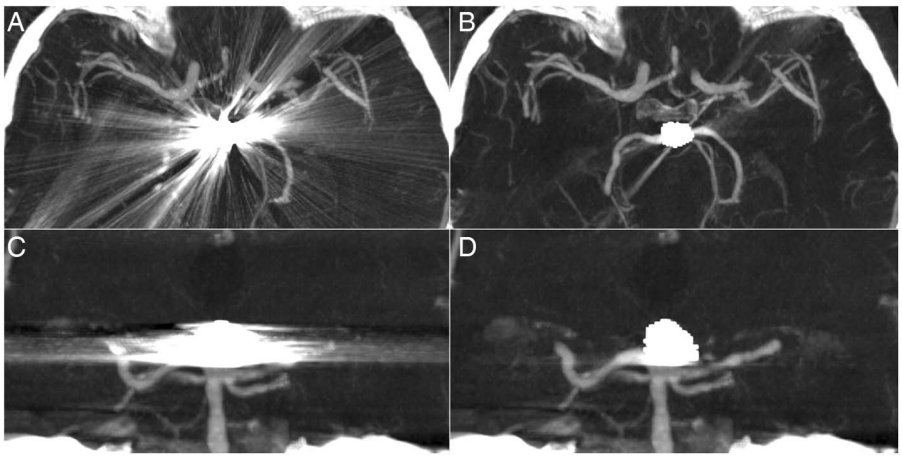

Figure 3 Axially (upper row) and coronally (lower row) reconstructed IV CT angiograms after coil embolization of a ruptured basilar tip aneurysm. The visibility of the adjacent posterior cerebral arteries improved significantly after metal artifact reduction (B and D).

the assessability of vascular structures after MAR (all $p \leq 0.063$ owing to the reduced number of cases available for statistical analysis in subgroups).

For the detection of aneurysm remnants, the number of diagnostic datasets increased from 4 to 19 (13% to 61%; McNemar test, $p<0.001$) for all treated aneurysms (n=31) after MAR. Thus, MAR enabled the detection of aneurysm remnants (various sizes ranging from minimal residual neck to significant central reperfusion) in nine cases. Subgroup analysis (clipped patients and patients who underwent coiling without stenting; each group n=12) showed improved assessability for both groups and both readers. However, owing to smaller sample size and differences in interpretation of images without MAR, significance levels for the two readers were heterogeneous (aneurysm clipping: reader 1: 2.0±0.0 vs 1.5±0.5; p=0.031; reader 2: 2.0±0.0 vs 1.67±0.5; p=0.125/aneurysm coiling: reader 1: 1.58±0.52 vs 1.33±0.4.9; p=0.375; reader 2: 2.0 ±0.0 vs 1.25±0.45; p=0.004).

The overall agreement for all cases between the two raters, however, was 80.7% with $\kappa=0.738$, indicating a substantial agreement.

In figure 1 the effects of MAR upon image quality are visualized, and representative follow-up cases after clipping, coiling, and stent-assisted coiling are shown in figures 2–4.

We also tried to improve the assessability of stented vessels by applying the MAR algorithm to the radiopaque stent markers (n=9). MAR, however, did not further improve the generally good assessability of stented vessels (figure 5), including the parts of the vessel adjacent to the radiopaque stent markers (McNemar, p=1.000). It is worth mentioning that our attempts to apply MAR to a Pharos stent and a Silk Plus flow diverter were unsuccessful and these stents became non-diagnostic after MAR. Although the artifacts caused by a WEB device were relatively low, our attempt to apply MAR improved assessability of the aneurysm lumen (not shown).

The mean time (±1 SD) required for post-processing (including manual definition of the radiopaque materials and subsequent automatic application of MAR) was 11.8±2.3 min (range 7–16 min) and depended on the number and size of objects marked for MAR.

DISCUSSION

Owing to its high resolution, C-arm based flat panel detector CT has been used to assess cerebrovascular structures and implants used to treat cerebrovascular pathologies.[15 16] Furthermore, angiography systems allowing flat-panel detector CT have been used for the immediate evaluation of complications, such as periprocedural hemorrhage.[5 17] Unfortunately, even small radiopaque objects like clips or coils often cause significant beam hardening artifacts at the level of the implants, thereby hampering analysis of the adjacent brain parenchyma and cerebrovasculature. To deal with this problem, different algorithms to reduce artifacts from metallic implants have been implemented.[18–24] For example, Yu *et al*[25] presented a segmentation-based interpolation method to reduce the metal artifacts caused by surgical aneurysm clips, whereas Wang and coworkers applied a fusion based prior image approach.[26] Prell *et al* developed an interpolation-based three-dimensional (3D)

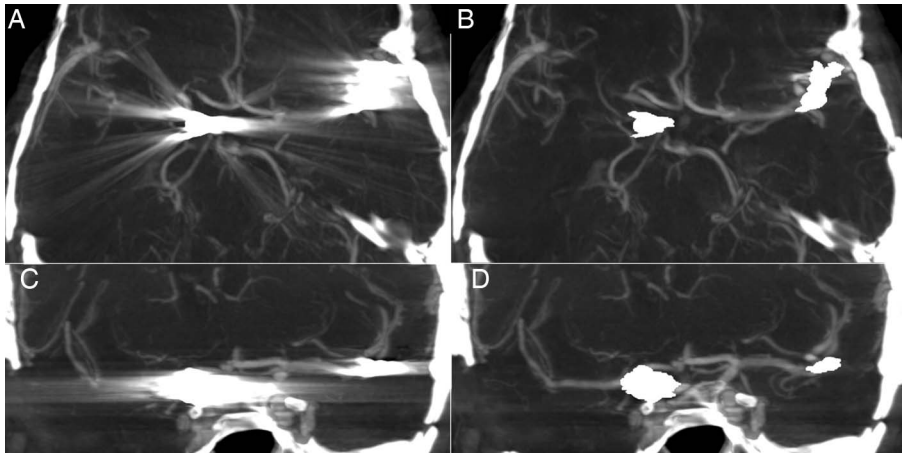

Figure 4 Axial (upper row) and coronal (lower row) IV CT angiogram reconstructions of a patient who underwent coil embolization of a ruptured right-sided posterior communicating artery aneurysm and subsequent clipping of an innocent left-sided middle cerebral artery (MCA) aneurysm. Metal artifact reduction (B and D) clearly improved assessability of the MCA and its branches.

Pjontek R, *et al*. *J NeuroIntervent Surg* 2016;**8**:824–829. doi:10.1136/neurintsurg-2015-011787

J NeuroIntervent Surg: first published as 10.1136/neurintsurg-2015-011787 on 7 September 2015. Downloaded from http://jnis.bmj.com/ on July 7, 2022 by guest. Protected by copyright.

Figure 5 Follow-up images of a patient who underwent stenting of a symptomatic high-grade stenosis of the right middle cerebral artery (MCA) using an Enterprise stent. The radio-opaque stent endings which barely cause artifacts (A) coarsened after metal artifact reduction (MAR) (B). Consequently, the visibility of the stent lumen at the endings minimally worsened after MAR.

correction algorithm for the raw data.[12 13] In our study we used an improved version of the interpolation-based MAR algorithm described Prell *et al*. Another difference in our study compared with other studies is that our data were acquired during a 20 s rotational flat panel scan without subtraction, whereas other work groups applied, for example, shorter subtraction-based acquisition protocols.[27 28]

Consistent with previous studies the application of MAR clearly reduced the metal artifacts, leading to a significantly improved assessability of vascular structures and aneurysm remnants, which are the most relevant elements for clinical decision-making.[11 29–31] The number of datasets with adequate visibility of the parent vessel and potential aneurysm remnants, however, did not reach the level of the series published by Psychogios *et al*.[29] Considering the relatively small cohort of their study and ours, the observed difference does not automatically imply a worse performance of the MAR algorithm in our study, but might have been influenced by several factors such as imaging protocol, size, and orientation of coil masses or clips in relation to the parent vessel or subjective criteria of the observers for sufficient assessability.

The severity of metal artifacts and thus the effect on image quality depends on the kind, size, and material of the implant. The improvement of image quality and clinical assessability after MAR is more distinct in cases with larger amounts of implanted material—for example, multiple clips or large coil packages. For aneurysm remnants, however, MAR did not improve the assessability in a number of cases with larger coilings. For such cases time-of-flight MR angiography might as well be used for follow-up imaging.

For implanted intracranial stents MAR did not improve stent visibility or depiction of the parent vessel, as the applied intracranial stents caused barely any artifacts and therefore the surrounding tissue did not benefit from MAR. Assessability of the vessel lumen in these cases was unproblematic. Although proximal or distal radiopaque markers were associated with local metal artifacts in some stents (eg, Enterprise stent), we found that application of MAR to these markers did not further improve image quality (figure 5).

For the clinical acceptance of a product, such as the software used for MAR, the reconstruction time is an important parameter. We found that the complete post-processing time ranged between 7 and 16 min, depending on the number of objects being marked for MAR and the size of the dataset. In comparison with the time required for reconstruction of a normal CT, these times are quite long and one would prefer online MAR. These relatively long times are required because several consecutive optimization steps are performed by the software, of which the last one can be shortened at the operator's discretion. On the other hand, once the metallic objects have been defined the workstation can be left alone during the calculations. Further optimization of the software used and an increase in computer performance are expected to solve this problem soon, with MAR being expected to become used routinely.

Limitations

Although our cohort provides the highest number of implants after MAR in a single study, the small number of cases is a shortcoming of this study, and new devices were underrepresented (eg, only one flow diverting stent and one intra-aneurysmal flow diverter). On the other hand, studies separately analyzing the applicability of IV CTA for intra-aneurysmal flow diverters have been published recently.[15 32 33] Furthermore, we did not quantitatively analyze image quality. However, the informative value of Hounsfield units (HU) or signal-to-noise-ratio measurements may be controversial since the artifacts show inter- and intraindividual heterogeneity. Consequently, the HU values depend strongly on the size and on the placement of a region-of-interest (primary hyperdense vs hypodense area). Moreover, the clinical impact of the quantitative analysis is clearly inferior to the qualitative assessment. Furthermore, we did not distinguish between different clip materials (eg, cobalt or titanium alloy), and we did not calculate the total length or number of the implanted platinum coils. This, on the other hand, allows the transfer our results to a 'normal' clinical setting. Finally, a direct comparison of the MAR and non-MAR IV CTA with (3D-) DSA images would have been desirable. However, as the main point was to investigate the improvements of IV CTA due to MAR and since we only infrequently performed 3D-DSA routinely in our patients at times close to that at which IV CTA was performed, we did not compare IV CTA with DSA.

CONCLUSION

The prototype MAR software significantly improves image quality of IV contrasted angiographic CT datasets in patients after coiling or clipping and thereby results in significantly improved diagnostic value of IV CTA images in this patient group.

Contributors All authors participated in drafting the article and revising it critically for important intellectual content. All authors made substantial contributions to conception and design, acquisition of the data, and analysis and interpretation of the data. All authors provided final approval of the version to be published.

Funding This work was supported by Siemens AG (Healthcare).

Disclaimer The concepts and information presented in this paper are based on research and are not yet completely commercially available.

Competing interests The authors MW and MAB received travel grants and speaker honorarium from Siemens Healthcare, Germany.

Ethics approval Local ethics committee of the University Hospital of the RWTH Aachen.

Provenance and peer review Not commissioned; externally peer reviewed.

J NeuroIntervent Surg: first published as 10.1136/neurintsurg-2015-011787 on 7 September 2015. Downloaded from http://jnis.bmj.com/ on July 7, 2022 by guest. Protected by copyright.

Data sharing statement Unpublished anonymized data may be available on request.

Open Access This is an Open Access article distributed in accordance with the Creative Commons Attribution Non Commercial (CC BY-NC 4.0) license, which permits others to distribute, remix, adapt, build upon this work non-commercially, and license their derivative works on different terms, provided the original work is properly cited and the use is non-commercial. See: http://creativecommons.org/licenses/by-nc/4.0/

REFERENCES

1 Raymond J, Guilbert F, Weill A, *et al*. Long-term angiographic recurrences after selective endovascular treatment of aneurysms with detachable coils. *Stroke* 2003;34:1398–403.
2 Campi A, Ramzi N, Molyneux AJ, *et al*. Retreatment of ruptured cerebral aneurysms in patients randomized by coiling or clipping in the International Subarachnoid Aneurysm Trial (ISAT). *Stroke* 2007;38:1538–44.
3 Kaufmann TJ, Huston J III, Mandrekar JN, *et al*. Complications of diagnostic cerebral angiography: evaluation of 19,826 consecutive patients. *Radiology* 2007;243:812–9.
4 Kau T, Hauser M, Obmann SM, *et al*. Flat detector angio-CT following intra-arterial therapy of acute ischemic stroke: identification of hemorrhage and distinction from contrast accumulation due to blood-brain barrier disruption. *AJNR Am J Neuroradiol* 2014;35:1759–64.
5 Arakawa H, Marks MP, Do HM, *et al*. Experimental study of intracranial hematoma detection with flat panel detector C-arm CT. *AJNR Am J Neuroradiol* 2008;29:766–72.
6 Heran NS, Song JK, Namba K, *et al*. The utility of DynaCT in neuroendovascular procedures. *AJNR Am J Neuroradiol* 2006;27:330–2.
7 Shinohara Y, Sakamoto M, Takeuchi H, *et al*. Subarachnoid hyperattenuation on flat panel detector-based conebeam CT immediately after uneventful coil embolization of unruptured intracranial aneurysms. *AJNR Am J Neuroradiol* 2013;34:577–82.
8 Finkenstaedt T, Morsbach F, Calcagni M, *et al*. Metallic artifacts from internal scaphoid fracture fixation screws: comparison between C-arm flat-panel, cone-beam, and multidetector computed tomography. *Invest Radiol* 2014;49:532–9.
9 Kau T, Rabitsch E, Celedin S, *et al*. Feasibility and potential value of flat-panel detector-based computed tomography in myelography after spinal surgery. *J Neurosurg Spine* 2009;10:66–72.
10 Stidd DA, Theessen H, Deng Y, *et al*. Evaluation of a metal artifacts reduction algorithm applied to postinterventional flat panel detector CT imaging. *AJNR Am J Neuroradiol* 2014;35:2164–9.
11 van der Bom IM, Hou SY, Puri AS, *et al*. Reduction of coil mass artifacts in high-resolution flat detector conebeam CT of cerebral stent-assisted coiling. *AJNR Am J Neuroradiol* 2013;34:2163–70.
12 Prell D, Kalender WA, Kyriakou Y. Development, implementation and evaluation of a dedicated metal artefact reduction method for interventional flat-detector CT. *Br J Radiol* 2010;83:1052–62.
13 Prell D, Kyriakou Y, Struffert T, *et al*. Metal artifact reduction for clipping and coiling in interventional C-arm CT. *AJNR Am J Neuroradiol* 2010;31:634–9.
14 Meyer E, Raupach R, Lell M, *et al*. Normalized metal artifact reduction (NMAR) in computed tomography. *Med Phys* 2010;37:5482–93.
15 Caroff J, Mihalea C, Neki H, *et al*. Role of C-arm VasoCT in the use of endovascular WEB flow disruption in intracranial aneurysm treatment. *AJNR Am J Neuroradiol* 2014;35:1353–7.
16 Buhk JH, Kallenberg K, Mohr A, *et al*. Evaluation of angiographic computed tomography in the follow-up after endovascular treatment of cerebral aneurysms–a comparative study with DSA and TOF-MRA. *Eur Radiol* 2009;19:430–6.
17 Dorfler A, Struffert T, Engelhorn T, *et al*. Rotational flat-panel computed tomography in diagnostic and interventional neuroradiology. *RoFo* 2008;180:891–8.
18 Watzke O, Kalender WA. A pragmatic approach to metal artifact reduction in CT: merging of metal artifact reduced images. *Eur Radiol* 2004;14:849–56.
19 Zhao S, Robertson DD, Wang G, *et al*. X-ray CT metal artifact reduction using wavelets: an application for imaging total hip prostheses. *IEEE Trans Med Imaging* 2000;19:1238–47.
20 Wang G, Frei T, Vannier MW. Fast iterative algorithm for metal artifact reduction in X-ray CT. *Acad Radiol* 2000;7:607–14.
21 Wang G, Snyder DL, O'Sullivan JA, *et al*. Iterative deblurring for CT metal artifact reduction. *IEEE Trans Med Imaging* 1996;15:657–64.
22 Ebraheim NA, Coombs R, Rusin JJ, *et al*. Reduction of postoperative CT artifacts of pelvic fractures by use of titanium implants. *Orthopedics* 1990;13:1357–8.
23 Kalender WA, Hebel R, Ebersberger J. Reduction of CT artifacts caused by metallic implants. *Radiology* 1987;164:576–7.
24 Glover GH, Pelc NJ. An algorithm for the reduction of metal clip artifacts in CT reconstructions. *Med Phys* 1981;8:799–807.
25 Yu H, Zeng K, Bharkhada DK, *et al*. A segmentation-based method for metal artifact reduction. *Acad Radiol* 2007;14:495–504.
26 Wang J, Wang S, Chen Y, *et al*. Metal artifact reduction in CT using fusion based prior image. *Med Phys* 2013;40:081903.
27 Golitz P, Struffert T, Ganslandt O, *et al*. Contrast-enhanced angiographic computed tomography for detection of aneurysm remnants after clipping: a comparison with digital subtraction angiography in 112 clipped aneurysms. *Neurosurgery* 2014;74:606–13; discussion 13–4.
28 Golitz P, Struffert T, Kaschka I, *et al*. Optimized angiographic CT using intravenous contrast injection: a noninvasive imaging option for the follow-up of coiled aneurysms? *AJNR Am J Neuroradiol* 2014;35:2341–7.
29 Psychogios MN, Scholz B, Rohkohl C, *et al*. Impact of a new metal artefact reduction algorithm in the noninvasive follow-up of intracranial clips, coils, and stents with flat-panel angiographic CTA: initial results. *Neuroradiology* 2013;55:813–8.
30 Hung SC, Wu CC, Lin CJ, *et al*. Artifact reduction of different metallic implants in flat detector C-arm CT. *AJNR Am J Neuroradiol* 2014;35:1288–92.
31 Buhk JH, Groth M, Sehner S, *et al*. Application of a novel metal artifact correction algorithm in flat-panel CT after coil embolization of brain aneurysms: intraindividual comparison. *Rofo* 2013;185:824–9.
32 Struffert T, Lang S, Adamek E, *et al*. Angiographic C-arm CT visualization of the Woven EndoBridge cerebral aneurysm embolization device (WEB): first experience in an animal aneurysm model. *Clin Neuroradiol* 2014;24:43–9.
33 Saake M, Struffert T, Goelitz P, *et al*. Angiographic CT with intravenous contrast agent application for monitoring of intracranial flow diverting stents. *Neuroradiology* 2012;54:727–35.

J NeuroIntervent Surg: first published as 10.1136/neurintsurg-2015-011787 on 7 September 2015. Downloaded from http://jnis.bmj.com/ on July 7, 2022 by guest. Protected by copyright.